Microphase Structures of Poly(styrene-*b*-ethylene/propylene) Diblock Copolymers Investigated by Solid-State NMR and Small-Angle X-ray Scattering Techniques

Hongshi Yu,[†] Jiahu Wang,[†] Almeria Natansohn,*[,†] and Marsha A. Singh[‡]

Departments of Chemistry and Physics, Queen's University, Kingston, Ontario, Canada K7L 3N6

Received January 26, 1999

ABSTRACT: The microphase structures of two commercial polystyrene-*b*-poly(ethylene/propylene) diblock copolymers with different compositions and molecular weights have been studied by solid-state NMR and small-angle X-ray scattering (SAXS) techniques. The nearly homogeneous narrow proton line shape of the rubber peaks in the two-dimensional wide-line separation (WISE) spectrum indicates that the interfacial region between the rigid polystyrene and the mobile rubber phases is small compared with the size of the domains. ^{1}H spin diffusion measurements were used to measure the sizes of various domains and the interface between them using a model that considers the effects of ^{1}H spin−lattice relaxation. The thickness of the interface determined by NMR is about 2 nm for both copolymers. Interdomain distances measured by NMR agree well with the results of SAXS measurements and increase with the increase of the molecular weight of the copolymers. However, the sizes of dispersed polystyrene domains obtained from NMR are smaller than the values from SAXS. This may be caused by the model differences used in interpreting the data from these two methods. This combined approach greatly increases the reliability of the findings and confirms the validity of the simulation model used in the NMR data analyses.

1. Introduction

Most important industrial polymers are multicomponent phase-separated systems. Adding rubber to polystyrene can produce a two-phase material with polystyrene in the matrix phase and rubber in the dispersed phase. The impact strength of this material is greater than that of polystyrene itself. Generally speaking, block copolymers are phase-separated systems that often exhibit unique and useful properties as a consequence of the general thermodynamic incompatibility of the blocks. These multiphase block copolymers are not only useful by themselves but also can be used as compatibilizers for immiscible blends. The degree of mixing, characterized by the size of the dispersed phase and the thickness of the interfacial region, is crucial to many mechanical and optical properties exhibited by these multicomponent materials.

Various experimental techniques, each with advantages and disadvantages, are available to investigate the heterogeneity in these materials. The differential scanning calorimetry (DSC) technique has been widely used to study the miscibility of copolymers and polymer blends. Incompatible systems show distinct separate glass transition temperatures.[1,2] However, DSC is only sensitive to domain sizes larger than about 10 nm.[3,4] Scanning electron microscopy (SEM) is useful as a probe of the morphological structure with domain sizes above a few tens of nanometers but cannot reliably resolve structures smaller than 10 nm. The resolution for transmission electron microscopy (TEM) is higher than that of SEM. However, it is still not easy to get reliable data for domain sizes below 10 nm. In addition, TEM cannot be used for polymer materials for which no suitable stain reagents can be found.[5] Neutron scattering and fluorescence spectroscopy require special synthetic methods in order to obtain data on the phase structure. Small-angle X-ray scattering is a powerful method to study the phase separation process and determine microdomain sizes. However, in general, accurate SAXS measurement of interdomain spacing requires relatively monodisperse samples and long-range ordering of the domain structures as well as a relatively high degree of electron density contrast between phases.

High-resolution solid-state NMR offers new possibilities for studying the microphase structure of heterogeneous polymers.[6−14] In contrast to scattering techniques, the NMR techniques do not depend on the existence of periodic structure in the sample. Furthermore, unlike TEM, no sample treatment to enhance the contrast between the two components is needed. As a high-resolution and nondestructive method, NMR is a powerful, but still not conventional, tool to be used for quantitative determination of domain sizes of materials. Therefore, it is important to use a number of techniques simultaneously to characterize the sample microstructures and verify the reliability of the NMR results.

The proton spin−lattice relaxation times in the laboratory [T_1(H)] and in the rotating frame [$T_{1\rho}$(H)] are sensitive to heterogeneity in the materials. The latter has been used as a convenient probe to identify the separated minority phase at a level of a few nanometers. The two-dimensional heteronuclear wide-line separation (WISE) NMR techniques[13,15] can be used to obtain information about molecular dynamics in a phase-separated system. For every ^{13}C resonance, WISE yields a proton wide-line spectrum which reflects the dipolar couplings of protons in the proximity of the ^{13}C nucleus. A WISE experiment establishes a correlation between the microphase structure and segmental mobility in the probed system. In addition, various spin diffusion techniques have also been used to probe chemical or physical heterogeneities in polymer systems.[6−14] A

[†] Department of Chemistry.
[‡] Department of Physics.
* Corresponding author.

10.1021/ma990106i CCC: $18.00
Published on Web 06/10/1999

Scheme 1. Chemical Structure of the SEP Sample

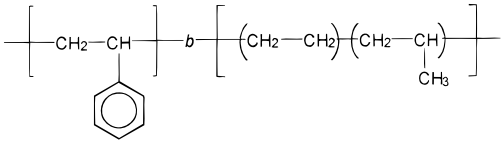

Poly(styrene) Poly(ethylene/propylene) (EP)

Table 1. Characterization of the SEP Sample

sample code	weight ratio (PS/R)	volume fraction of PS	total M_w (kg/mol)	M_w of the S block (kg/mol)	poly-dispersity
SEP-1	32/68	0.288	144	46	1.20
SEP-2	26/74	0.224	218	57	1.17

dipolar filter pulse sequence[16] (based on mobility differences) may be used to select the magnetization of one component in a two-component system. During the following mixing time, the magnetization will migrate from the selected component to the initially suppressed region. This magnetization transfer proceeds until the system reaches equilibrium. The rate of spin diffusion reflects the mixing level of the probed system and can be employed to extract the microphase parameters such as domain sizes and interfacial thickness.[17]

At the boundary between the two phases in a copolymer material there are normally regions with gradually changing composition, the so-called interfaces. The nature and sizes of these interfaces have attracted considerable attention. A few models have been developed[18,19] to extract information about interfaces from solid-state NMR measurements. From the spin diffusion point of view, a system with an interface can be considered as consisting of three regions: source, sink, and interface. With given initial conditions, the spin diffusion process, which is measured by NMR experiments, can be numerically simulated. This procedure leads to the determination of domain size and interfacial thickness parameters in the system.

In this paper, the microphase structures of two commercial elastomer polystyrene-*block*-poly(ethylene/propylene) diblock copolymers have been investigated by solid-state NMR and small-angle X-ray scattering techniques. Results from the $T_{1\rho}$(H), T_1(H), two-dimensional WISE, spin diffusion, and SAXS measurements are presented. The microphase parameters are obtained by simulating the spin diffusion process, and the calculated results are compared with those obtained by small-angle X-ray scattering. Comparisons of the observed spin−lattice relaxation time [T_1(H)] with the simulated spin−lattice relaxation time are also made.

2. Experimental Section

2.1. Samples. Kraton G1701X and Kraton G1702X are poly(styrene-*b*-ethylene/propylene) (SEP) (see Scheme 1) diblock copolymers which were generously provided by the Shell Company. The weight ratios of the polystyrene and the rubber in the samples are 37/63 and 28/72 as calculated from ^{1}H NMR in $CDCl_3$ solution. In the following, the abbreviations "SEP-1" and "SEP-2" will be used for these two systems, respectively. The poly(ethylene/propylene) is a hydrogenated polyisoprene block and is completely amorphous. The molecular weights, M_w's, and polydispersities for both samples, determined by GPC, are listed in Table 1. Two separate glass transition temperatures, 103 °C/−36 °C for SEP-1 and 105 °C/−26 °C for SEP-2, were recorded by DSC on a Mettler TC 10A system at a scanning rate of 20 °C /min.

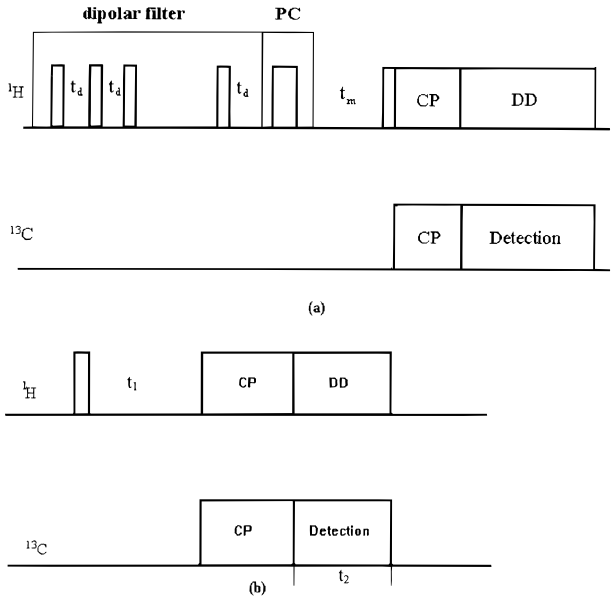

Figure 1. Pulse sequences used in the spin diffusion experiments: (a) dipolar filter pulse sequence;[16] (b) WISE pulse sequence.[13]

2.2. NMR Measurements. The solid-state NMR measurements were made on a Bruker ASX-200 spectrometer operating at 200 and 50.29 MHz for ^{1}H and ^{13}C, respectively. The sample was spun at 3.3 kHz in order to avoid overlapping of the spinning sidebands and the other peaks. The $\pi/2$ ^{1}H pulse lengths were about 3.7−4.2 μs. An optimum contact time of 1.5 ms was used for all the measurements except for the WISE experiment. The ^{13}C spectra were obtained using the methods of cross-polarization, magic angle spinning, and dipolar decoupling (CP-MAS/DD). All spectra were obtained at room temperature.

Proton spin−lattice relaxation times in the rotating frame [$T_{1\rho}$(H)] were measured using carbon detection in a pulse sequence with an increasing proton spin locking time. In the two-dimensional WISE experiment, 512 points were used in the carbon domain and 64 points in the proton domain with increments of 4 μs. A short 300 μs contact time was used for the carbon detection in order to avoid spin diffusion during cross-polarization.

The dipolar filter pulse sequence was used for both T_1(H) and spin diffusion measurements. In the T_1 experiment, complete suppression of the spin magnetization in the entire system was achieved using 300 μs delays between the pulses in the filter, and the filter was repeated five times. The recovery of magnetization then gave T_1(H) for all the carbon peaks. Phase cycling (PC, an alternation of a π pulse or no pulse) was not used in this measurement. In the spin diffusion case, selection of the mobile component was achieved using cycles of 12 $\pi/2$ proton pulses repeated seven times and with 12 μs delays between the pulses. PC was used to eliminate the T_1(H) effect in the spin diffusion process. The dipolar filter[16] and the WISE[13] pulse sequences are shown in Figure 1.

2.3. SAXS Measurements. Small-angle X-ray scattering (SAXS) measurements were made using both in-house and synchrotron facilities. In-house data were obtained with a Rigaku special fine-focus Cr tube source to provide a line-shaped initial beam of 8 mm height and 0.15 mm width. A flat pyrolytic graphite monochromator, in conjunction with a series of beam shaping slits, was used to select the Cr Kα energy (λ = 2.29 Å). The diffractometer is operated in transmission mode with a 1-dimensional solid-state position-sensitive detector (Princeton Instruments Inc. X-PDA1024) having 1024 photodiodes (pixels) of 2 mm height and 25.4 μm center-to-center distance. A total exposure of 12 h was allowed for each measurement with ongoing subtraction of the pixel dark count. The scattering profiles were corrected for back-

ground (parasitic scattering from slits, windows, and air) by subtracting normalized profiles obtained using a similar setup in the absence of the sample.

The resolution of the in-house data was 624 pixels/deg with a minimum scattering angle of 0.05° or 2.39×10^{-3} Å^{-1}. The second value is the momentum transfer, q, defined as $q = (4\pi \sin \theta)/\lambda$), where 2θ is the scattering angle. Following preliminary smoothing of the data,[20] the smearing effect of the finite beam height was corrected using the direct desmearing method.[21]

Synchrotron data for the SEP samples were obtained at beamline D11A-SAXS of the Laboratório Nacional de Luz Síncrotron (LNLS) located in Campinas, Brazil.[22] A 1-dimensional delay line detector was used with a sample-to-detector distance of 1.5 m and a wavelength of 1.6 Å. Five minute exposures were used with background correction provided by a measure of the scattering in the absence of the sample. The background data were normalized using transmission ratios obtained with a NaI scintillation detector placed in line with the main beam after Co and Al attenuators. The possibility of detector artifacts occurring at positions near the primary beam was noted, and the synchrotron data interpretation is therefore limited to the high-q range of scattering angles.

3. Results and Discussion

Two separate glass transition temperatures were obtained from the thermal analysis. This indicates that the material has separated phases, and the domain sizes are probably larger than 10 nm.[3,6,23]

3.1. Spin-Lattice Relaxation and WISE Experiments Studies. The proton spin−lattice relaxation time in the laboratory frame, T_1(H), and in the rotating frame, $T_{1\rho}$(H), can be used to estimate the microphase structure of a heterogeneous polymer system. Each parameter provides qualitative information about the phase sizes at different levels. Spin diffusion leads to an averaging effect on the $T_{1\rho}$(H)'s or T_1(H)'s of the different components. In a homogeneous system, a single spin−lattice relaxation time is observed. For heterogeneous systems, more than one $T_{1\rho}$(H) and/or T_1(H) values are usually found because there is insufficient time for spin diffusion to equilibrate the magnetization in the different phases. Separate $T_{1\rho}$(H)'s and T_1(H)'s have often been used as indications of the lack of miscibility, and the actual values can be used to estimate upper or lower limits of domain sizes.

In Figure 2 the SEP-1 sample CPMAS spectrum and the assignment of each peak are shown. Signals 1 and 2 belong to the aromatic carbons in polystyrene. The aliphatic carbons of the polystyrene contribute to signal 3. Signals 4−7 come from different carbons in the rubber. For each resolved signal, the $T_{1\rho}$(H) and T_1(H) values were measured, and the results are summarized in Table 2. All signals from the rubber give one set of $T_{1\rho}$(H) and T_1(H) values while all signals from the PS give another set of $T_{1\rho}$(H) and T_1(H) values. The existence of different $T_{1\rho}$(H)'s and T_1(H)'s indicates that the system is heterogeneous at both $T_{1\rho}$(H) and T_1(H) probing levels. The T_1's of polystyrene and rubber homopolymers of comparable molecular weights have been measured and are 1600 and 230 ms, respectively. These values are taken as the respective intrinsic T_1's for polystyrene and rubber in the copolymer. It is evident that spin diffusion leads to a partial averaging of the two T_1(H)'s. This implies that spin diffusion and spin−lattice relaxation occur at comparable rates in this system.[24] The $T_{1\rho}$(H)'s and T_1(H)'s of the SEP-2 are also given in Table 2.

The two glass transition temperatures and the different $T_{1\rho}$'s and T_1's for both systems indicate different

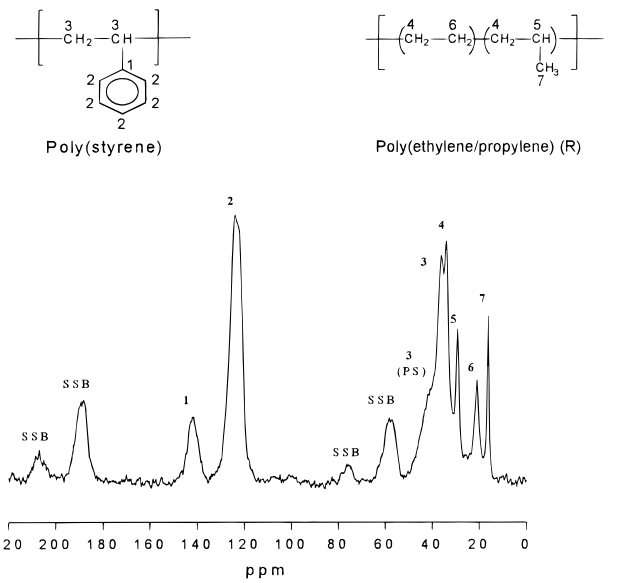

Figure 2. ^{13}C CP/MAS NMR spectrum of SEP-1 sample. SSB is a spinning sideband.

Table 2. $T_{1\rho}$(H) and T_1(H) Data of the SEP Samples

sample code	$T_{1\rho}$ (ms) of S block	$T_{1\rho}$ (ms) of EP block	T_1 (ms) of S block	T_1 (ms) of EP block
SEP-1	6.8 ± 0.5	2.2 ± 0.2	484 ± 20	251 ± 5
SEP-2	7.2 ± 0.4	2.5 ± 0.5	448 ± 30	298 ± 10
S			1600 ± 100	
EP				230 ± 20

mobilities for the two components in the materials: the rigid polystyrene and the mobile EP rubber components. As mentioned in the Introduction, in general, there should be an interfacial region in which a partial mixing of the incompatible chain segments occurs, as suggested by Meier[25] in 1973, Hashimoto et al.[26] in 1974, and Helfand[27] in 1975. Previous experimental studies indicate the existence of such an interface in many polystyrene-containing block copolymers: poly(styrene−methyl methacrylate) (PS−PMMA),[28] poly(styrene−isoprene) (PS−PI),[29−31] and poly(styrene−methylphenylsiloxane) (PS−PMPS).[10] A few methods, such as SAXS and NMR, have been used to characterize the interface. Schmidt-Rohr et al. demonstrated that the 2D wide-line separation (WISE) experiment is a good method to determine the mobility at the interface and measure interfacial thickness approximately in poly(styrene−dimethylsiloxane) (PS−PDMS) and PS−PMPS systems.[13] Protons in a mobile component display motional narrowed peaks while those from a rigid phase exhibit broad peaks. For the PS−PDMS system, the highly mobile PDMS signal does not show any significant fraction of a broad polystyrene component, and the interfacial thickness has been estimated to be smaller than 1 nm. On the other hand, the PS−PMPS system shows a narrow and a broad component in the proton line shape of the methyl signal, and about 50% of the PMPS exhibits a significantly reduced mobility. This indicates that a relatively large interface exists between the two components. Very recently, similar studies for polyureas (with soft−rigid components) have been reported, and significant heterogeneous proton line shapes have been found for both the rigid and the soft components,[32] which indicates that the systems contain immobilized soft segments as well as mobile hard segments. Details about the WISE technique and its interpretation can be found in ref 13.

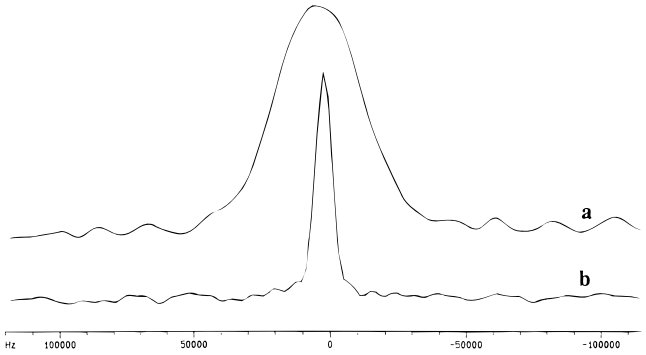

Figure 3. Two slices taken from SEP-1 WISE contour spectrum: (a) 127 ppm, (b) 25 ppm.

Because of close contact with the rigid PS, it is reasonable to assume that the EP rubber in the interface, surrounding the rigid PS phase, is less mobile than the rubber in the bulky rubber phase. If the amount of immobilized EP rubber is significant compared with the total amount of the rubber, it will show a broader component in the narrow proton spectrum. To see these mobility changes in the interface, 2D WISE spectra of SEP samples were obtained, and a slice from the PS at 127 ppm and a slice from the EP at 25 ppm taken from the SEP-1 contour spectrum are shown in Figure 3. To minimize spin diffusion during cross-polarization (CP), a CP time of only 300 μs was used. Quantitative analysis was not attempted, but a clear mobility difference in Figure 3 between the rigid polystyrene phase and the mobile rubber is readily apparent. Unlike PS−PMPS, in which a significant broad component could be found underneath the mobile PMPS, the highly mobile EP rubber component shows a nearly homogeneous narrow peak with no significant broad component, while the aromatic PS shows a very broad line and no narrow component is seen. These results indicate that neither significant immobilized soft segments nor mobile hard segments exist in the SEP samples. Since only those systems that have a significant interfacial region compared with the sizes of the domains have been reported to show the features in the WISE spectrum (such as PS−PMPS[13] and polyureas[32] systems), then these results do not necessarily mean that there is no interface between the rigid PS and the mobile EP segments. This may indicate that the percentage of more mobile aromatic PS and of immobilized EP rubber is not significant, and the interfacial region may be small compared with the size of the domains. To determine the actual phase sizes and interfacial thickness, spin diffusion measurements were carried out.

3.2. Spin Diffusion Measurements. The significant differences in mobility between polystyrene and the rubber allow us to apply the dipolar filter pulse sequence[16] to differentiate the two phases. As shown in Figure 1, the dipolar filter consists of 12 $\pi/2$ proton pulses which are separated by a delay time t_d. If a relatively long delay time is used and the cycle repeated several times, the rigid component decays quickly and cannot be refocused by the following pulse sequence. The mobile component is then selected by the dipolar filter pulse sequence. Through spin diffusion, the proton magnetization in the rigid phase will gain from the proton magnetization in the mobile phase during the mixing time, t_m, and is recorded through ^{13}C detection. In Figure 4, a series of ^{13}C spectra at different t_m values for SEP-1 are displayed. For the shortest t_m (50 + 750 μs) (750 μs is half of the cross-polarization time because spin diffusion also occurs during this time period), only signals from the rubber component are detected. With increasing t_m, signals from the polystyrene component appear, and their intensities increase. At the same time the intensities of the rubber peaks decrease. The spin−lattice relaxation leads to magnetization contributions that cannot be distinguished from those of spin diffusion. Its effect can be reduced by a simple alternation of a π pulse and no pulse before the mixing time (PC). If the selected proton magnetization is aligned along $+z$ and $-z$ axes in alternating scans, most of the T_1 relaxation contribution is canceled. The application of phase cycling causes all of the observed signals to decrease in intensity at long mixing times. In the following data treatment, the intensities at different mixing times were corrected by multiplying a factor of $\exp(t_m/T_1)$. As mentioned in section 3.1, two T_1(H) values were found in these materials (Table 2). The T_1(H) of the polystyrene component (484 ms) for SEP-1 was used to correct the intensity of the polystyrene signal in Figure 4, and the results are shown in Figure 5 as solid dots. The same treatment has been performed for the SEP-2 (not shown here).

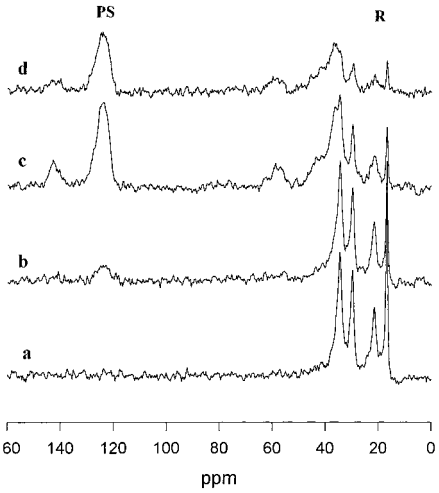

Figure 4. Dipolar filter spectra of SEP-1 at different mixing time: (a) 50 μs, (b) 5 ms, (c) 150 ms, and (d) 400 ms.

3.3. Simulations of the Spin Diffusion Measurements. With the above spin diffusion curves, the magnetization recovery of the PS peak as a function of mixing time, one can obtain domain size information by using an initial-rate approximation with the assumption of a narrow interface formed between the rigid PS and mobile EP rubber.[18] However, accurate quantitative determination of the domain size requires a numerical simulation of the spin diffusion curves.

In solid-state NMR experiments, a nuclear spin experiences Zeeman interaction with the static magnetic field and dipolar interaction with other spins in the system. Therefore, the signal intensity recovery for those initially suppressed peaks depends on both spin−lattice relaxation and spin diffusion. The spin diffusion process is sensitive to the microphase structure, and as such it can be used to determine domain sizes and interfacial thickness of the phase-separated system.[18,19] The rate of spin−lattice relaxation is characterized by the numerical values of T_1(H). The observed T_1(H)'s, 484 ms for polystyrene and 251 ms for rubber, are partially averaged in comparison with the intrinsic T_1(H)'s (see

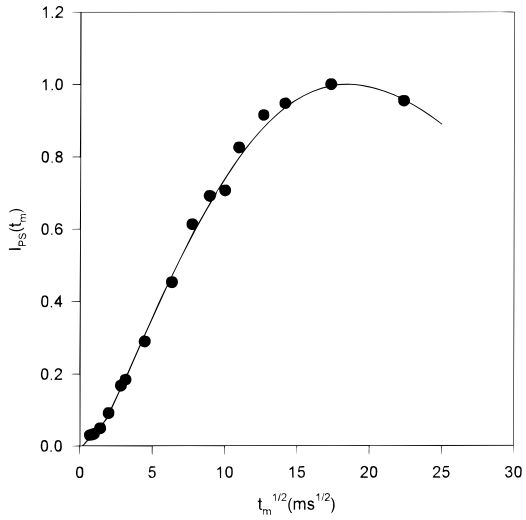

Figure 5. Magnetization growth of the protonated aromatic carbon of polystyrene for SEP-1 sample as a function of mixing time using the dipolar filter method. The solid dots are experimental data. The fitting parameters are the polystyrene domain $d_{PS} = 27$ nm, the interphase $d_1 = 2$ nm, and the long period $d_R = 53$ nm.

Table 2). This implies that spin diffusion and spin−lattice relaxation proceed at comparable rates. Therefore, a model that treats both processes on an equal footing[24] was used for the numerical simulation. The combined spin diffusion and spin−lattice relaxation can be described by the following diffusion equation:

$$\frac{\partial c_z^A(r,t_m)}{\partial t_m} = D_A \Delta c_z^A(r,t_m) + \frac{c_z^\infty - c_z^A(r,t_m)}{T_{1A}} \qquad (1)$$

where $c_z^A(r,t_m)$ is the specific spin magnetization, D_A is the spin diffusion coefficient, and T_{1A} is the intrinsic spin−lattice relaxation time in phase A. c_z^∞ is the equilibrium value of the specific spin magnetization in the system. A similar equation exists for the B phase. The above two equations should be solved with proper initial and boundary conditions as outlined in a previous publication.[19]

The total spin magnetization in each phase, which is proportional to the NMR signal intensity, can be conveniently obtained by integrating the specific spin magnetization over the respective region, Ω_A or Ω_B, i.e.,

$$M_z^A(t_m) = \rho_H^A \int_{\Omega_A} c_z^A(r,t_m)\, dr \qquad (2)$$

where ρ_H^A is the proton density in phase A.

Equation 1 is general for systems where diffusion coefficients and T_1 values are constant in each of the domains and can be applied to simulate T_1(H)'s in a phase-separated polymer with a given microphase structure by choosing the appropriate initial conditions. In this model, the composition of the interface is assumed to change linearly from one domain to another. This can be translated to a linear change of the spin diffusion coefficient and proton density. The intrinsic relaxation rate ($1/T_1$) also goes through a linear change within the interface.

$$\frac{1}{T_1} = \frac{f_A}{T_{1A}} + \frac{1 - f_A}{T_{1B}} \qquad (3)$$

where f_A is the molar fraction of phase A. Details of this spin diffusion and spin−lattice relaxation model and numerical treatment can be found elsewhere.[19,24]

It can be seen from eq 1 that the spin diffusion coefficient, D, is one of the important parameters in the numerical simulation. Therefore, knowledge of the spin diffusion coefficient is a prerequisite for accurately characterizing the domain sizes. In general, the domain size is proportional to the square root of the spin diffusion coefficient. If D is known, the fit procedure will yield the domain sizes. On the other hand, if the domain sizes are well characterized by other methods, the fit will give the spin diffusion coefficient D.

It has been demonstrated that the spin diffusion coefficient D is proportional to the strength of the dipolar couplings and to the square of the average distance between the nearest protons, r_{HH}. The strength of the dipolar coupling is proportional to the full width at half-height, $\Delta\nu_{1/2}$, of a proton line in a ^{1}H wide-line spectrum. The resulting proportionality relation is

$$D \sim \Delta\nu_{1/2}(r_{HH})^2 \qquad (4)$$

However, the relationship between the spin diffusion coefficient D and the proton line width[33] is not simply linear. The resulting discrepancy in the spin diffusion coefficient determined only by proton line width may preclude quantitative estimation of the domain sizes in some applications. Two studies have focused on the calibration of the spin diffusion coefficient, D, by fitting the spin diffusion data with parameters from a set of known domain structures.[18,33] This is one method to determine spin diffusion coefficient D, and the results can be compared with those estimated from proton line width measurements.

Clauss et al.[18] have performed spin diffusion measurements on a set of PS-*b*-PMMA block copolymer samples which are well characterized by SAXS and TEM techniques. The domain sizes, obtained from SAXS and TEM, have been used to fit the spin diffusion curves, and a spin diffusion coefficient of 0.8 nm^2/ms for the PS and the PMMA components has been determined. This value is used in this paper for the polystyrene block. In another study, a polystyrene-*b*-polybutadiene block copolymer previously characterized by TEM has been used to calibrate the spin diffusion coefficient, D, and a value of 0.05 nm^2/ms has been determined for the mobile polybutadiene.[33] To determine the D value for the EP rubber, the well-defined SAXS microdomain structures of a series of PS-hydrogenated polyisoprene block copolymers have been used to fit the spin diffusion curves, and a D value of 0.1 nm^2/ms was determined[34,35] for the mobile EP rubber phase which reasonably agrees with a roughly 190 Hz proton line width.

It also can be seen from eq 1 that solutions for the diffusion process will depend on dimensionality or morphologies of the materials. It has been established, especially by TEM, SEM, and SAXS, that segregated microphases can be three-dimensional spheres, two-dimensional cylinders, or one-dimensional lamellae. To determine the morphologies of the systems, SEM has been attempted, but the samples appear to be homogeneous at the 100 nm scale resolution. This is also an indication that the domain size of the system may be below 100 nm. As the domain morphologies of block copolymers have been studied extensively, particularly

Table 3. Some Parameters of the SEP Sample

phase	proton fraction	density, g/cm^3	proton density, g/cm^3	diffusion coeff, nm^2/ms	dimensionality
PS	0.077	1.06	0.081	0.8	2
rubber	0.143	0.89	0.127	0.1	2

Scheme 2. Schematic Two-Dimensional Representation of the Three-Dimensional Model Used in the NMR Simulation (S = PS Domains; I = Interfacial Region; EP = EP Rubber Domains)

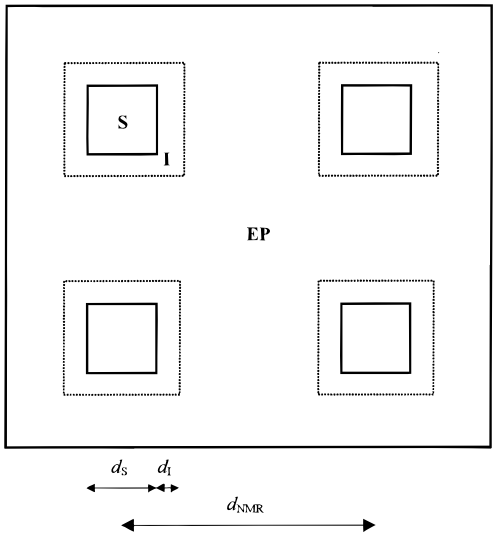

for styrene−diene block copolymers, and depend primarily upon the fractional composition of the dispersed phase, we assume that cylindrical domains for the dispersed polystyrene, which are often observed for phase-separated block copolymer systems of similar composition,[36,37] are arranged in a two-dimensional hexagonal lattice for both SEP materials, based on the compositions given in Table 1. The dimensionality and other information used in the simulation are given in Table 3.

Although a cylindrical domain arrangement in a hexagonal lattice is thought to better describe the true morphology of the materials, it is difficult to use such a model to simulate the spin diffusion curve because of two reasons. One is the long time required at the present computational power; the other one is the complexity of choosing this kind of model. As discussed before, the spin diffusion equation (1) for one-dimensional systems can be solved with suitable initial and boundary conditions. For two-dimensional systems, the solutions can be expressed as the products of one-dimensional solutions. If a dispersed cylinder domain arrangement in a hexagonal lattice were chosen in the simulation model, a complicated boundary condition would be expected and therefore adds much more difficulty to solve the spin diffusion equations. For simulation simplicity, we assume a rectangular parallelepiped with a square base in a two-dimensional simple square lattice arrangement formed in the rubber matrix, and a schematic two-dimensional representation of this model is given in Scheme 2. As reported by many authors, the initial slower increase of intensity in the dipolar filter experiment (Figure 5) further suggests the presence of a small interface between the polystyrene and the rubber phases.[16,19,38] Therefore, in our model, the microphase structure of the sample is assumed to consist of a polystyrene square, surrounded by an interface, and then a continuous rubber phase. The area of each square represents the volume fraction of the corresponding domain. For a given set of microphase structure parameters, two separate simulations with different initial conditions were performed. The first one corresponds to the process in which the data are collected immediately after the dipolar filter pulse, and the initial magnetization for the source and sink are 1 and 0, respectively. The second one is related to the data collecting process after a π pulse and the initial magnetization of the source and sink are −1 and 0, respectively. The difference of magnetization in the PS (or rubber) region from the above two simulations, when multiplied by a factor $\exp(t_m/T_1)$, is directly comparable with the experimental data obtained using phase alternation. To obtain the microstructure of the samples, the domain size of PS, d_{PS}, and the interfacial thickness, d_I, have been changed independently to fit the spin diffusion curve. It has been found that the spin diffusion curve is sensitive to the various domain size parameters. The best fitting parameters which can obtain for SEP-1 and SEP-2 are summarized in Table 4. The uncertainties in each parameter in the table are estimated from the fitting process. Domain size parameters chosen outside of the uncertainty range give a poor fitting. For example, if the interfacial thickness value is chosen to be $d_I = 3.0$ nm or $d_I = 1.0$ nm (outside of $d_I = 2.0 \pm 0.5$ nm), there are visible differences in the magnetization growth curves when compared to the experimental curves. The best fit curve for the SEP-1 sample is shown as a solid curve in Figure 5 with the inner polystyrene domain size, $d_{PS} = 27$ nm, and the interface, $d_I = 2$ nm. The long period, the distance between two adjacent polystyrene squares, is $d_L = d_{PS} + 2d_I + d_R = 53$ nm. An interface of a similar size has been reported in other polystyrene−rubber block copolymers[29,31,39,40] by other techniques. The agreement between experiment and simulation is quite good for both copolymers. The simulations by the model, including the effects of the spin−lattice relaxation, capture the basic features of the spin diffusion curves: the sigmoidal shape of the experiment and the signal intensity from polystyrene increasing slowly at the beginning and reaching the maximum at $t_m^{1/2} \approx 17$ ms$^{1/2}$ and then decaying because of T_1 effects. As discussed by Wang et al.[24] and Jack et al.,[31] only the simulation model which includes the effects of the spin−lattice relaxation reproduces the decrease of the magnetization after a maximum point, which agrees with the experimental results for SEP samples. Without including the spin−lattice relaxation, one has to use an overestimated interface to fit the spin diffusion curves.[24] For our samples, the interfacial thickness would be 3−4 nm if simulated by previous models.[19] As we discussed in the WISE experiment, it seems that a relatively smaller interfacial region is more appropriate for our samples. This may also indicate that the results obtained by a simulation model including the T_1 effects

Table 4. Domain Sizes d_{PS}, d_I, d_L and Simulated T_1(H) of the Polystyrene Block and EP Rubber Block for the SEP-1 and SEP-2 Samples

sample code	d_{PS} (nm) ± 1 nm	d_I (nm) ± 0.5 nm	d_L[a] (nm) ± 2.4 nm	T_1(H) (ms) of S block	T_1(H) (ms) of EP block
SEP-1	27	2	53	430	264
SEP-2	28	2	63	444	252

[a] $d_L = d_{PS} + 2d_I + d_R$.

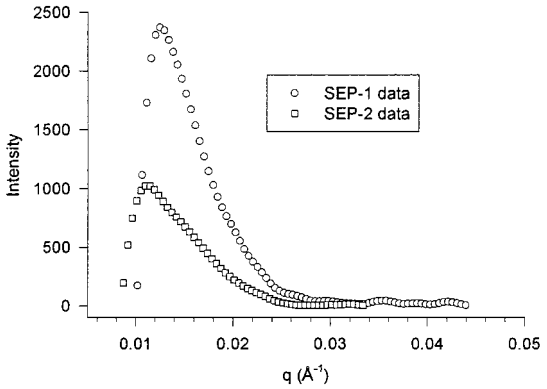

Figure 6. Desmeared SAXS scattering intensity distribution as a function of scattering angle for SEP sample.

are more accurate than those by the pure spin diffusion model.

If we assume that half of the interface contains polystyrene of increased mobility and other half consists of the immobilized EP rubber, and taking into account the estimated domain size of polystyrene of 27 nm, 2 nm interfacial thickness, and 53 nm long period, the percentages of the polystyrene and the rubber in the interface will be about $[(27 + 1)^2 - 27^2]/(27 + 1)^2 = 7\%$ of total polystyrene and about $[(27 + 2)^2 - (27 + 1)^2]/[53^2 - (27 + 1)^2] = 3\%$ of the total rubber based on the simulation model in the Scheme 2. The 3% of EP rubber of reduced mobility may be not enough to show a significant broad component underneath of the narrow rubber proton peak in the WISE experiment. It is much less than that of poly(methylphenylsiloxane) published by Schmidt-Rohr et al.,[13] where about 50% poly(methylphenylsiloxane) exhibits immobility and shows a significant broad component in the proton line shape. It is also much less than that of polyurea systems,[32] where the interfacial thickness is about 2 nm while the domain size is about 3 nm. From the results presented here, it appears that the WISE experiment can provide information on the mobility changes in the interface only for those systems that have a relatively significant interfacial region compared with the sizes of the domains.

With the microphase structure determined above, the simulation of T_1 curves for the PS and the rubber domains was carried out using the solution of eq 1 with different initial conditions. The least-squares fitting for an exponential function was then used to determine the T_1 values, and the results obtained are 430 and 264 ms for polystyrene and rubber for SEP-1, respectively; they are reasonably close to the corresponding measured values of 484 and 251 ms. These simulated T_1(H) determined by NMR for SEP-1 and SEP-2 are also summarized in Table 4.

3.4. SAXS Measurements Studies. *Domain Spacings.* The desmeared scattering patterns of the SEP-1 and SEP-2 materials exhibit primary interaction peaks at scattering angles of 0.0125 and 0.0115 Å^{-1}, respectively (Figure 6). There is no evidence of long-range ordering in the form of multiple Bragg peaks. The observed scattering maxima can therefore be interpreted as a result of average interparticle distances of 61 ± 3 and 67 ± 3 nm, respectively, resulting from short-range order interactions. This is obtained using the known relation[41] between an average particle spacing, d_{av}, and the location of a scattering maximum in a disordered system, q_{max}.

$$d_{av} = 1.22a, \quad \text{where } a = 2\pi/q_{max} \tag{5}$$

Here a would be the distance interpreted in the context of the Bragg equation for an ordered system, the lattice constant. With this interpretation, the effective lattice spacing (a) corresponding to the observed peaks would be 50 and 55 nm for the SEP-1 and SEP-2 samples.

For a well-ordered system with multiple diffraction peaks, Sakurai et al.[42] have discussed the relation between the interparticle distance and the Bragg spacing in terms of their morphology in their recent published paper. The interdomain distances are given by a for simple cubic, $(4/3)^{1/2}a = 1.15a$ for cylinders in a hexagonal lattice, and $(3/2)^{1/2}a = 1.22a$ for body-centered-cubic and face-centered-cubic symmetry. Therefore, it is reasonable to assume that the true interparticle spacings, the distance between adjacent polystyrene cores, lie within the ranges of 50−61 nm for SEP-1 and 55−67 nm for SEP-2.

Domain Sizes. In attempting to estimate the radius of gyration, R_g, of the scattering particles, Guinier plots in the form of ln(intensity) vs q^2 (q = momentum transfer) were generated. The Guinier approximation[43] states that a linear relation should be observed at sufficiently small angles with a slope of $-R_g^2/3$ for 3-dimensional globular particles. It is generally accepted that the useful angular range is limited to values of q where $qR_g < 1$.[43] A significant linear region was, indeed, observed in the Guinier plots, but only at angles higher than the interaction peaks occurring at 0.0125 and 0.0115 Å^{-1} in the two data sets. This observation is initially unexpected since no Guinier regions are predicted in the presence of significant interparticle interactions.

The nature of the linear Guinier plots was examined using a series of ideal scattering profiles generated for varying particle radius and concentration. The hard-sphere potential was assumed with a spherical particle scattering function.[44] For volume fractions where only a single short-range ordering peak is visible, an (effective) linear Guinier region can be identified within an estimated range $1.45 < qR_g < 2.60$. Given an ideal radius of gyration of 12 nm, the value of R_g estimated using a linear regression was found to be about 13.5 nm with a negligible fit error. The tendency to overestimate the particle radius of gyration at these higher angles is not significantly greater than what is seen at the smallest experimentally accessible angles for the ideal case of noninteracting particles. In addition, ideal particle sizes and measured results are seen to converge with finite polydispersity in the system. Guinier analysis at angles greater than the scattering maximum is therefore seen to be a valid tool for these systems.

Figure 7 shows the results of Guinier analyses of the in-house data yielding radius of gyration values of about 13.7 nm for the SEP-1 and 14.3 nm for the SEP-2 samples. The linearity of the Guinier plot can be interpreted as a partial confirmation of the 3-dimensional structure of the microdomains. No conclusions regarding the true shape, in terms of the particle anisometry, can be made with this analysis. If an approximately spherical shape is assumed, the radius of gyration values (R_g) correspond to a particle radius (r) of about 17.7 nm for SEP-1 and 18.5 nm for SEP-2, resulting from the following equation:

$$R_g^2 = (3/5)r^2 \tag{6}$$

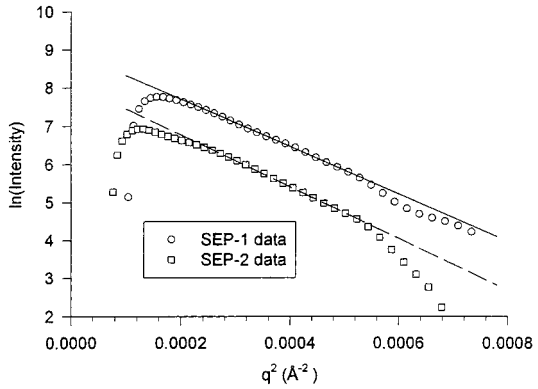

Figure 7. Guinier plot in the form of ln(intensity) as a function of the square of the scattering angle for SEP sample.

Table 5. Domain Size Results from SAXS

sample code	r^a (nm)	d^b (nm)	$R_a{}^c$ (nm)
SEP-1	17.7	35 ± 2	50−61 ± 3
SEP-2	18.5	37 ± 2	55−67 ± 3

[a] r is the radius of the polystyrene domain. [b] d is the diameter of the polystyrene domian. [c] R_a is the distance between the polystyrene domain.

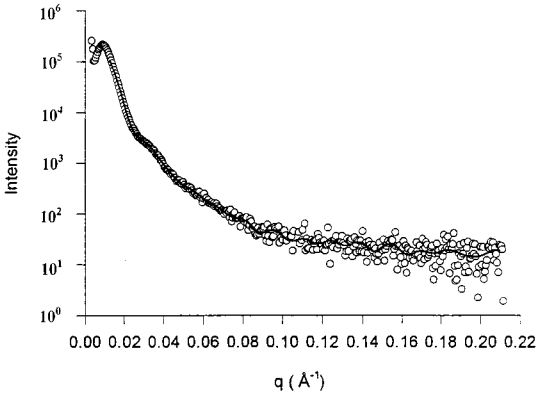

Figure 8. Synchrotron SAXS scattering intensity with indirect transform fit result for SEP-1. The circles are experimental data, and the solid line is the fit result.

Results are summarized in Table 5.

Pair Distribution Function. The synchrotron data on SEP-1 and SEP-2 samples were used primarily to examine the high-q scattering behavior using the method of indirect transformation[44] to fit the data and obtain real space information on the particle structure. Figure 8 shows the synchrotron data for the SEP-1 sample as circles with the solid line fit result drawn through the curve at values of q excluding the interaction peak.

The indirect transform method of small-angle scattering data treatment is much less sensitive to low-q information and provides a measure of the pair (distance) distribution function, $P(r)$, of the scattering objects. The $P(r)$ function can be interpreted as a measure of the frequency of a particular distance, r, separating volume elements within the particle. $P(r)$ must be therefore vanish for values of r larger than the largest dimension of the particle, d. A homogeneous sphere would exhibit a maximum in $P(r)$ at $r_{max} = 0.525d$, where d is the particle diameter.[43] The ratio of r_{max}/d can be seen to decrease with increasing deviation from the ideal 3-dimensional structure of the sphere. In particular, the $P(r)$ function for the SEP data shows clear evidence of distortion from a true spherical shape since the r_{max}/d ratios are 0.43 for the SEP-1 shown in Figure 9 and 0.41 for the SEP-2 sample. Quantitative estimates of the nature of the anisometry are not possible for particles that are still essentially 3-dimensional. However, it is reasonable to choose a prolate versus oblate ellipsoidal shape given the volume fraction of the copolymers.[36,37] The estimated values for R_g using this approach are about 14.9 nm for SEP-1 and 15.4 nm for the SEP-2 samples, in relatively good agreement with Guinier results for the in-house momentum q 13.7 and 14.3 nm, respectively.

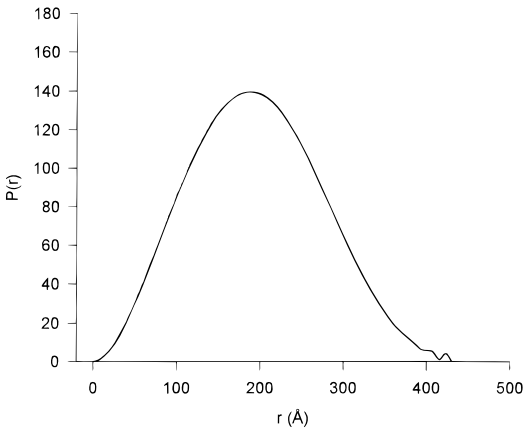

Figure 9. Pair distribution function obtained from the indirect transform fit to the synchrotron SAXS data for SEP-1 sample.

Porod Analysis. Porod analysis of the synchrotron data at high q showed no evidence of the presence of an interfacial thickness between the phases. However, Porod plots of Iq^4 versus q^4 show clear positive deviations from the ideal zero slope case.[43] This result is generally attributed to the presence of electron density inhomogeneities within the two phases occurring at length scales large relative to the molecular structure. The possibility of incomplete phase separation may well obscure the effects of a finite but small interfacial region. No estimate of the specific volume of the microdomains was attempted from the Porod analysis in the absence of measurements of the absolute scattering intensity or a useful estimate of the total scattering (the invariant, Q).

3.5. Comparison of the Results from NMR and SAXS Measurements. By comparing the results from the above two independent techniques, NMR and SAXS, it can be seen that the interdomain distances (or the long period) from the NMR technique lie well within the range of those from SAXS. These distances are found to increase with increasing molecular weights of the copolymers, in agreement with the prediction of equilibrium theory.[45−47] However, the confirmation of the 2/3 power law is not attempted as only two samples with a relatively small change in molecular weights have been measured. The thickness of the interface does not change with the increase of the molecular weights for our observed two samples, and these results are consistent with predictions of the equilibrium theory[45−47] and other experimental studies.[29,31,39] However, the sizes of dispersed polystyrene domains measured by NMR are smaller than those by SAXS techniques. This may be caused by the model differences used by solid-state NMR and SAXS methods.

First, the SAXS method considers a two-phase system—rigid polystyrene and mobile EP rubber—while the NMR simulation model contains three phases: the

rigid polystyrene, the mobile EP rubber, and the interface. Generally speaking, there should be a mixed region where both polystyrene and EP rubber coexist. Therefore, the domain sizes of the dispersed polystyrene phase determined by NMR technique using the three-phase model will be smaller than those determined by SAXS using the two-phase model which neglects the presence of polystyrene in the interface.

Second, since only a primary peak and no long-range ordering peaks were found from SAXS data profile, no morphological information is available directly. The domain sizes of the dispersed polystyrene phase were approximately obtained from the radius gyration with an assumption of a perfect sphere particle formed for the PS components. However, the synchrotron studies indicate that the shape of the PS domains in these two samples probably is an elongated sphere rather than a perfect sphere, but quantitative estimation of the nature of the anisometry is impossible. This finding is generally in agreement with the prediction from the compositions of the PS in the samples, a two-dimensional cylindrical structure for the dispersed PS phase. The main difference here is the length of the PS cylinder compared with the length of the cross-sectional axis. SAXS does not provide definitive information on the nature of the anisometry of the PS domain, and the domain sizes of the polystyrene obtained are actually an average of the length of the elongated axis and the cross-sectional axis. Even though the synchrotron studies indicate that the length of the elongated axis is not very large in comparison with the cross-sectional axis, this average is still larger than the cross-sectional axis and smaller than the length of the elongated axis. Therefore, the domain sizes obtained by SAXS in this way will tend to be overestimated. For the NMR simulation model, on the other hand, as we previously discussed, a rectangular parallelepiped with a square base of the dispersed phase arranged in a two-dimensional simple square lattice (Scheme 2) was assumed, and the domain sizes obtained are actually the unit lengths of the square. The block copolymer system strives to minimize the interfacial area while maintaining the appropriate bulk density in each microdomain, from the free energy point of view. The smaller circular surface cylinder is more appropriate to describe the actual system than the rectangular parallelepiped with a square base model. This is one of the possible errors introduced by the NMR simulation model. The square unit length obtained by the NMR simulation can be converted to a diameter of an equivalent circle using the relation

$$d_{PS}' = \frac{2d_{PS}}{\sqrt{\pi}} \tag{7}$$

where d_{PS} is the domain size determined by NMR method, yielding domain sizes for SEP-1 and SEP-2 as 30 and 32 nm, respectively. This means that the domain sizes obtained by the NMR method are minimal values while those obtained by the SAXS method are maximal values in this situation.

The other possible error introduced by the NMR simulation model is the assumption of a long rectangular parallelepiped with a square base PS arrangement in a two-dimensional simple square lattice rather than a more common two-dimensional hexagonal lattice. As is well-known, different packing lattices will have different interdomain spacing; therefore, the assumption made by our simulation model will introduce some errors in the estimation of the interdomain distance. In a simple square lattice, each dispersed PS rectangular parallelepiped domain has four nearest neighbors, while in a two-dimensional hexagonal lattice, six nearest neighbors are around each PS domain. Therefore, the spin diffusion process will be more efficient in a two-dimensional hexagonal lattice than in a simple square lattice for the same volume fraction of the dispersed phase. Consequently, the use of a simple square lattice in the simulation of the experimental curve will cause an underestimation of the interdomain distance. For a given volume fraction of the dispersed phase, the interdomain distance, d_L , from NMR using a simple square lattice can be converted to a hypothetical interdomain distance, d_L', assuming a hexagonal lattice formed for the dispersed domains using the relation

$$d_L' = \frac{\sqrt{2}}{\sqrt[4]{3}} d_L \approx 1.07 d_L \tag{8}$$

This means that about 7% error appears from the use of a simple square lattice rather than of a hexagonal lattice in the NMR simulation. However, this simple square lattice model is still generally accepted because the hexagonal lattice model is too complicated for the present computational power.

In addition, for an ideal two-dimensional cylinder packing system in the NMR simulation, we assume that no spin diffusion happens in the long cylindrical direction. In general, this is true for a long cylinder system with the length much greater than the cross-sectional axis. However, for relatively short cylinder systems, this assumption may also cause an underestimation of the domain sizes since nonnegligible spin diffusion in the short cylindrical direction will make the overall spin diffusion process more efficient.

4. Conclusions

The microdomain structures of two commercial block copolymers have been investigated by solid-state NMR and SAXS techniques. Two separate $T_{1\rho}$(H) values and T_1(H) values were observed, indicating separate phases. The 2D WISE spectra show that the mobilities of the polystyrene phase and of the rubber phase are very different. However, no significant broad component has been found for the narrow rubber proton line shape, which means that the interfacial region between the rigid PS and the mobile EP rubber is small. ^{1}H spin diffusion experiments have been used to determine the domain sizes and the interfacial thickness by simulating the experimental results with a model that considers the effects of ^{1}H spin−lattice relaxation time. It has been found that the spin diffusion curves are well reproduced by the simulation model for the two samples, and the agreement between the measured and simulated results is quite satisfactory. The simulations by the model including the spin−lattice relaxation term are more accurate than those by the pure spin diffusion model.

The interfacial region between polystyrene and EP rubber determined by the NMR method is about 2 nm for both samples. This is consistent with previous studies on a series of similar copolymers. The interdomain distances, determined by both NMR and SAXS methods, are found to increase with increasing of the molecular weights of the copolymer, and the NMR results fall well within the range suggested by the SAXS

results. However, the domain sizes of the PS blocks determined by NMR are smaller than those obtained by SAXS techniques. This discrepancy may be caused by the model differences used in the NMR and SAXS methods.

The spin−lattice relaxation time T_1(H) of the polystyrene and the rubber phase in the SEP samples changes significantly from those of their respective homopolymers. This change could be explained by the averaging effects of spin diffusion in the system. The predicted T_1(H)'s based on the microphase structure of the sample are close to the observed ones. This may mean that no significant differences in molecular motions occur in going from the homopolymer to this copolymer.

Acknowledgment. Support from the Natural Science and Engineering Research Council (NSERC) of Canada and the Environmental Science and Technology Alliance of Canada (ESTAC) is gratefully acknowledged. We thank Drs. Cho and Jack for helpful discussions. We also thank Dr. Greg Salomons and Mr. Tim Bardouille for assistance with the in-house SAXS measurements and the National Synchrotron Light laboratory (LNLS) in Brazil for the synchrotron SAXS measurements.

References and Notes

(1) MacKnight, W. J.; Karasz, F. E.; Fried, J. R. In *Polymer Blends*; Paul, D. R., Newman, D. R., Eds.; Academic Press: New York, 1978; Vol. 1.
(2) Paul, D. R.; Barlow, J. W.; Keskkula, H. In *Encyclopedia of Polymer Science and Engineering*; Mark, H. F., Bikales, N. M., Overberger, C. G., Menges, G., Eds.; John Wiley & Sons: New York, 1985; Vol. 12.
(3) Kaplan, D. S. *J. Appl. Polym. Sci.* **1976**, *20*, 2615.
(4) Walsh, D. J. In *Comprehensive Polymer Science*; Allen, G., Ed.; : Pergamon Press: Oxford, 1989; Vol. 2.
(5) Stamm, M. *Advances in Polymer Science*; Springer-Verlag: Berlin, 1992; Vol. 100, p 375.
(6) Schmidt-Rohr, K.; Clauss, J.; Blümich, B.; Spiess, H. W. *Magn. Reson. Chem.* **1990**, *28*, S3.
(7) Spiess, H. W. *Chem. Rev.* **1991**, *91*, 1321.
(8) Campbell, G. C.; VanderHart, D. L. *J. Magn. Reson.* **1992**, *96*, 69.
(9) Clauss, J.; Schmidt-Rohr, K.; Adam, A.; Boeffel, C.; Spiess, H. W. *Macromolecules* **1992**, *25*, 5208.
(10) Cai, W. Z.; Schmidt-Rohr, K.; Egger, N.; Gerharz, B.; Spiess, H. W. *Polymer* **1993**, *34*, 267.
(11) Cho, G.; Natansohn, A. *Can. J. Chem.* **1994**, *72*, 2255.
(12) Cho, G.; Natansohn, A.; Ho, T.; Wynne, K. J. *Macromolecules* **1996**, *29*, 2563.
(13) Schmidt-Rohr, K.; Clauss, J.; Spiess, H. W. *Macromolecules* **1992**, *25*, 3273.
(14) Schmidt-Rohr, K.; Spiess, H. W. In *Multidimensional Solid State NMR And Polymers*; Academic Press: London, 1994.
(15) Zumbulyadis, N. *Phys. Rev. B* **1986**, *33*, 6495.
(16) Egger, N.; Schmidt-Rohr, K.; Blümich, B.; Domke, W. D.; Stapp, B. *J. Appl. Polym. Sci.* **1992**, *44*, 289.
(17) Havens, J. R.; VanderHart, D. L. *Macromolecules* **1985**, *18*, 1663.
(18) Clauss, J.; Schmidt-Rohr, K.; Spiess, H. W. *Acta Polym.* **1993**, *44*, 1.
(19) Wang, J. *J. Chem. Phys.* **1996**, *104*, 4850.
(20) Brämer, V. R.; Wenig, W. *Kolloid Z. Z. Polym.* **1972**, *250*, 414.
(21) Singh, M. A.; Ghosh, S. S.; Shannon, R. F. *J. Appl. Crystallogr.* **1993**, *26*, 787.
(22) Kellermann, G.; Vicentin, F.; Tamura, E.; Rocha, M.; Tolentino, H.; Barbosa, A.; Craievich, A.; Torriani, I. *J. Appl. Crystallogr.* **1997**, *30*, 880.
(23) Xie, S.; Natansohn, A.; Rochon, P. *Macromolecules* **1994**, *27*, 1489.
(24) Wang, J.; Jack, K. S.; Natansohn, A. L. *J. Chem. Phys.* **1997**, *107* (3), 1016.
(25) Meier, D. J. In *Block and Graft Copolymers*; Burke, J. J., Weiss, V., Eds.; Syracuse University Press: New York, 1973.
(26) Hashimoto, T.; Nagatoshi, K.; Todo, A.; Hasegawa, H.; Kawai, H. *Macromolecules* **1974**, *7*, 364.
(27) Helfand, E. *Macromolecules* **1975**, *7*, 552.
(28) Zumbulyadis, N.; Landry, R.; Russell, T. P. *Macromolecules* **1996**, *29*, 2201.
(29) Tanaka, H.; Nishi, R. *J. Chem. Phys.* **1985**, *82*, 4326.
(30) Todo, A.; Hashimoto, T.; Kawai, H. *J. Appl. Crystallogr.* **1978**, *11*, 558.
(31) Jack, K. S.; Wang, J.; Natansohn, A.; Register, R. A. *Macromolecules* **1998**, *31*, 3282.
(32) Lehmann, S. A.; Meltzer, A. D.; Spiess, H. W. *J. Polym. Sci., Part B: Polym. Phys.* **1998**, *36*, 693.
(33) Spiegel, S.; Schmidt-Rohr, K.; Boeffel, C.; Spiess, H. W. *Polymer* **1993**, *34*, 4566.
(34) Jack, K S.; Natansohn, A.; Wang, J.; Favis, B. D.; Cigana, P. *Chem. Mater.* **1998**, *10*, 1031.
(35) Jack, K. S.; et al., manuscript in preparation.
(36) Quirk, R. P.; Fetters, L. J. In *Comprehensive Polymer Science*; Allen, G., Ed.; Pergamon Press: Oxford, 1989; Vol. 7.
(37) Riess, G.; Hurtrez, G.; Bahadur, P. In *Encyclopedia of Polymer Science and Engineering*; Mark, H. F., Bikales, N. M., Overberger, C. G., Menges, G., Eds.; John Wiley & Sons: New York, 1985; Vol. 2.
(38) VanderHart, D. L.; McFadden, G. B. *Solid State NMR* **1996**, *7*, 45.
(39) Hashimoto, T.; Shibayama, M.; Kawai, H. *Macromolecules* **1980**, *13*, 1660.
(40) Bates, F. S.; Berney, C. N.; Cohen, R. E. *Macromolecules* **1983**, *16*, 1101.
(41) Klug, H. P.; Alexander, L. E. *X-ray Diffraction Procedures*; John Wiley & Sons: New York, 1974; Chapter 12.
(42) Sakurai, S.; Kawada, H.; Hashimoto, T. *Macromolecules* **1993,** *26*, 5796.
(43) Feigin, L. A.; Svergun, D. I. *Structure Analysis by Small-Angle X-ray and Neutron Scattering;* Plenum Press: New York, 1987; Chapter 2.
(44) Svergun, D. I. *Appl. Crystallogr.* **1992**, *25*, 495.
(45) Helfand, E.; Wasserman, Z. R. *Macromolecules* **1976**, *9*, 879.
(46) Helfand, E.; Wasserman, Z. R. *Macromolecules* **1978**, *11*, 960.
(47) Helfand, E.; Wasserman, Z. R. *Macromolecules* **1980**, *13*, 994.

MA990106I